# Chapter 5

# Physical Properties of a Mesogenic Mixture Showing Induce Smectic $A_d$ Phase I: Refractive Index, Density, X-ray Diffraction and Static Dielectric Permittivity Studies

## 5.1 Introduction:

The induced Sm $A_d$ phase has been observed in bicomponent mixtures when none of the components of this mixture have smectic phase [1-7]. Generally, induced smectic phases are formed in binary mixtures of nematogenic compounds, one having terminal polar group and other being terminal non-polar one and only in a few cases [8-9], with mixtures of two non-polar mesogens. The strong induction of smectic $A_d$ phase is also possible in binary mixtures of polar nematic compounds as well [10-11]. Although, a considerable volume of work have been reported in the literature on systems involving polar non-polar mixtures of biphenyl compounds showing induced smectic phase, not much work have been done on binary systems of cyclohexane compounds showing induced smectic phase.

In this work, I have chosen a binary mixture of 4-n-pentyl phenyl 4-n′-hexyloxy benzoate (ME6O.5) and p-cyanophenyl trans-4-pentyl cyclohexane carboxylate (CPPCC). The pure compounds show nematic phase only. For a proper understanding of the formation of induced smectic phase and their influence on the adjacent nematic phase the physical properties of the mixture were studied by DSC, refractive index, density, x-ray diffraction and static dielectric permittivity measurements. The details of experimental technique employed are described in chapter 2 of this thesis. Phase transitions were studied by observing textures under a polarizing microscope equipped with Mettler FP80/82 thermo-system.

## 5.2 Texture study:

The compounds ME6O.5 and CPPCC were gifted by E. Merck, U.K. and were used without further purification. The transition temperatures of the pure compounds, their structural formula and chemical names are as follows:-

Component 1: p-cyanophenyl trans-4-pentyl cyclohexane carboxylate (CPPCC in short)

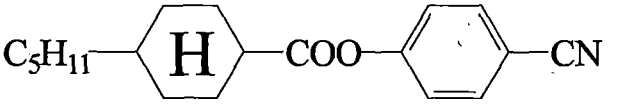


$$K \underset{21.4^{\circ}C}{\overset{48.7^{\circ}C}{\rightleftharpoons}} N \xrightarrow{80.5^{\circ}C} I$$

Component 2: 4-n-pentyl phenyl 4-n'-hexyloxy benzoate (ME6O.5 in short)

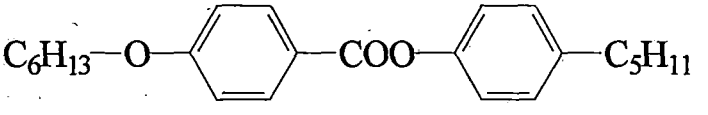


$$K \underset{35.5^{\circ}C}{\overset{49.5^{\circ}C}{\rightleftharpoons}} N \xrightarrow{62.5^{\circ}C} I$$

Of the eight mixtures, two show only nematic phase and all other have both nematic and induced smectic $A_d$ phases. During heating the smectic range is very small. The mixtures show large super-cooling. The induced smectic phase in this system appears mostly in the supercooling temperature region.

## 5.3 Phase diagram:

The phase diagram of this system is shown in figure 5.1. A detailed study of the phase diagram by microscopic observation revealed that the transition temperatures are reproducible within ±0.5°C between heating and cooling cycles for all the mixtures.

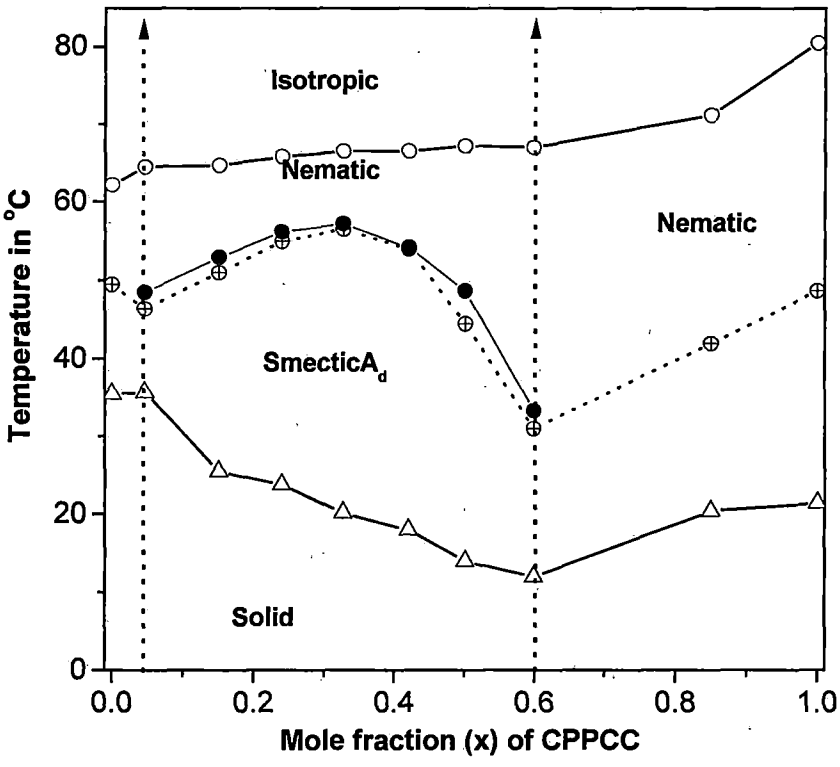


**FIGURE 5.1:** Phase diagram for the binary system of ME6O.5 + CPPCC. x is the mole fraction of CPPCC. ○ nematic-isotropic transition temperature; ● smecticA$_d$-nematic transition temperature; ⊕ melting temperature; △ super-cooling temperature.

The nematic–isotropic and smecticA–nematic transition temperatures are plotted against concentration. The mixture shows an induced smectic $A_d$ phase in the concentration range $0.03 < x < 0.6$, where x is the mole fraction of CPPCC. Maximum stability of the smectic phase occurs for mixtures

having $x \approx 0.3$. While Das et al for binary systems of similar benzoate esters and bi-phenyl compounds (5CB) [4-6] have found maximum stability of induced smectic phase near equimolar concentration.

The mixtures show large super-cooling. The super cooling temperatures show a minimum near $x \sim 0.6$. During heating the smectic range is very small for the mixtures within the concentration range $0.03 < x < 0.6$. The isotropic transition temperatures for mixtures having $x > 0.15$, lie significantly below the straight line connecting those of the pure compounds. Textures of the pure compounds and their mixtures in nematic phases show typical-marbled type and those in the induced smectic phases are fan-shaped or focal-conic, both typical of smectic A phase. Homeotropic texture studies also confirmed the existence of orthogonal phase in the induced smectic region.

## 5.4 DSC measurements:

In figure 5.2 the results of the transition entropy are plotted as a function of molar concentration ($x_{CPPCC}$). The change in entropy during smectic $A_d$ – nematic phase transition ($\Delta S_{SN}$) is larger for $x < 0.33$ compared to mixtures having $x > 0.33$. With increase in concentration of CPPCC above $x = 0.33$ there is a rapid decrease in $\Delta S_{SN}$, which suggest that for $x > 0.33$ the order of S-N phase transition is different from that for $x < 0.33$.

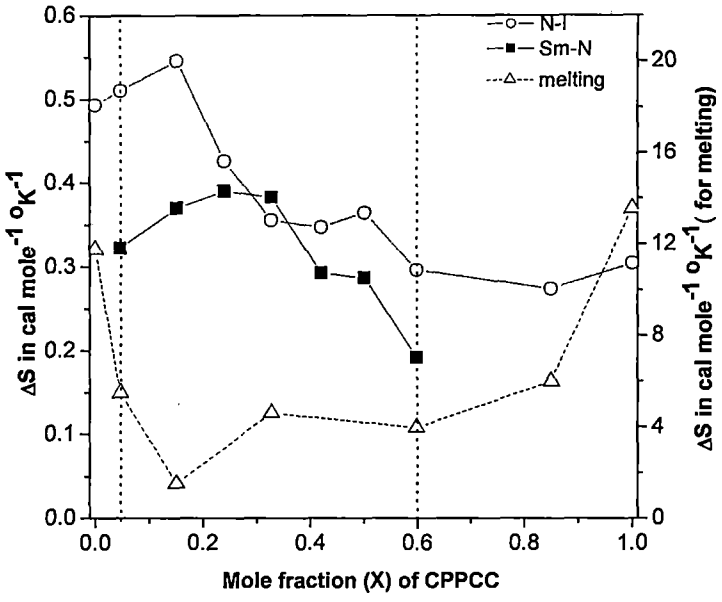


**FIGURE 5.2.** Transition entropies (ΔS) as a function of mole fraction of CPPCC: ■ smectic $A_d$ - nematic transition, ○ nematic-isotropic transition, and △ crystal-mesomorphic transition.

The entropy change associated with the nematic-isotropic phase transition ($\Delta S_{NI}$) however, decreases with increasing molar concentration ($x_{CPPCC}$), which indicates that the nematic phase of this system is relatively disordered with increase in the mole fraction of CPPCC. It is to be noted that for all the mixtures $\Delta S_{NI}$ values are higher compared to $\Delta S_{SN}$. It appears from the graph that ΔS values for crystal-mesomorphic transition decreases with increasing concentration (x) having a broad minimum near x=0.3.

## 5.5 Density measurements:

The temperature variation of the density values for the mixtures is shown in figure 5.3(a) – 5.3(b). A small discontinuity in the density values could be observed at the nematic to smectic $A_d$ phase transition for mixtures around a

mole fraction near x ≈ 0.3, consistent with the observed entropies of transition.

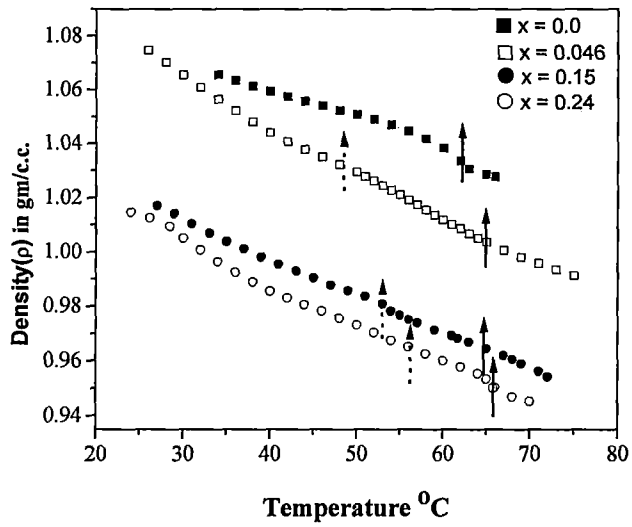


**FIGURE 5.3 (a).** Variation of density (ρ) as a function of temperature for x = 0.0, 0.046, 0.15, 0.24. ↑ nematic – isotropic and ↑ smectic $A_d$ – nematic transition temperatures.

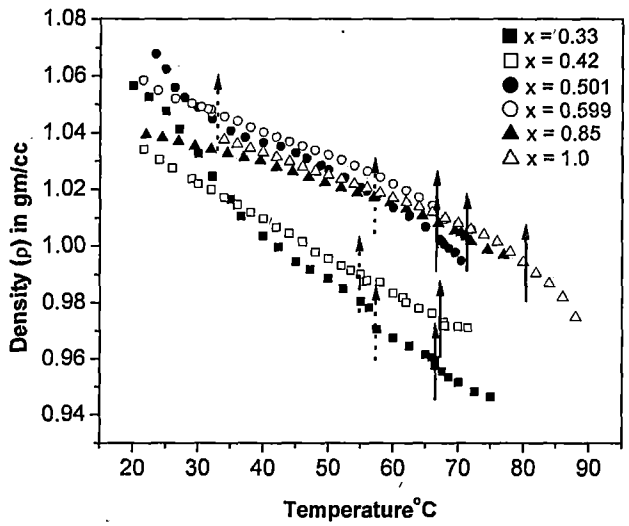


**FIGURE 5.3 (b).** Variation of density (ρ) as a function of temperature for x = 0.33, 0.42, 0.501, 0.599, 0.85, 1.0. ↑ nematic – isotropic and ↑ smectic $A_d$ – nematic transition temperatures.

## 5.6 Refractive index measurements:

The temperature dependence of the principal refractive indices $n_o$ and $n_e$ and the refractive index in the isotropic phase ($n_{iso}$) at wavelength $\lambda = 5780Å$ are shown in figures 5.5(a) – 5.5(e). In general, the change in birefringence is continuous for $x > 0.33$ at the smectic-nematic phase transition which indicates a very weakly first order or a second order phase transition. On the other hand for mixtures with $x < 0.33$ a discontinuity of birefringence ($\Delta n = n_e - n_o$) occurs at the smectic-nematic phase transition which indicates a first order phase transition. This observation is also supported by the density and transition entropy measurements of these mixtures.

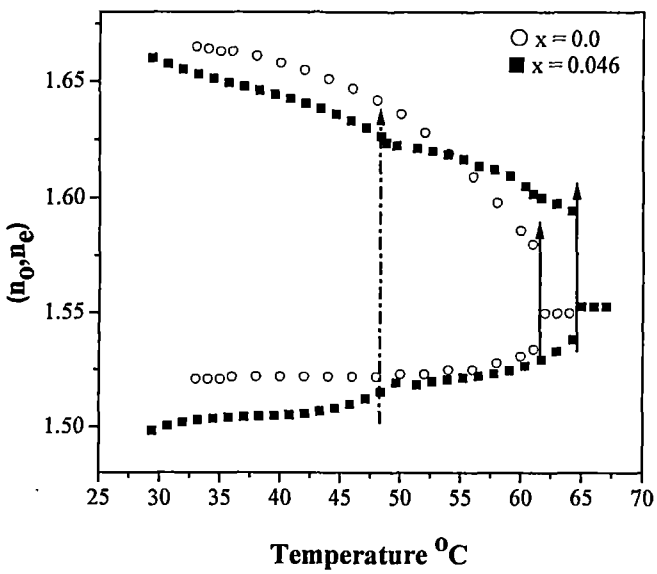


**FIGURE 5.5 (a).** Temperature variation of refractive indices ($n_o$, $n_e$) for ○ x = 0.0, ■ x = 0.046. ↑ nematic – isotropic and ↑ smectic $A_d$ – nematic transition temperatures

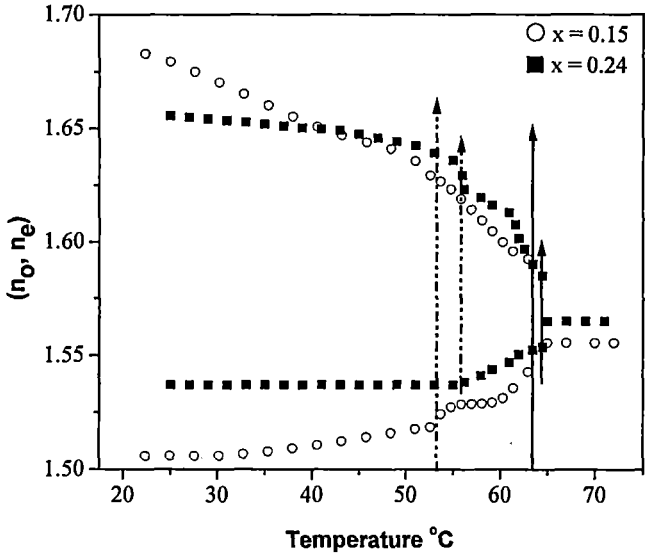


**FIGURE 5.5 (b).** Temperature variation of refractive indices ($n_o$, $n_e$) for ○ x = 0.15, ■ x = 0.24. ↑ nematic – isotropic and ↟ smectic $A_d$ – nematic transition temperatures

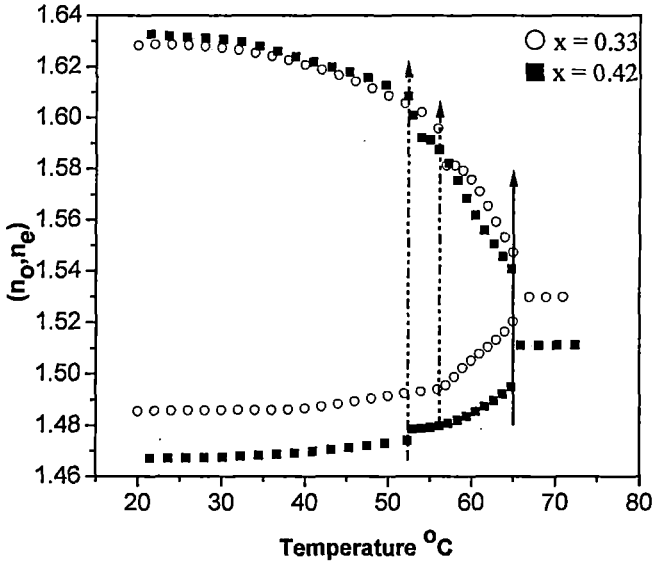


**FIGURE 5.5 (c).** Temperature variation of refractive indices ($n_o$, $n_e$) for ○ x = 0.33, ■ x = 0.42. ↑ nematic – isotropic and ↟ smectic $A_d$ – nematic transition temperatures

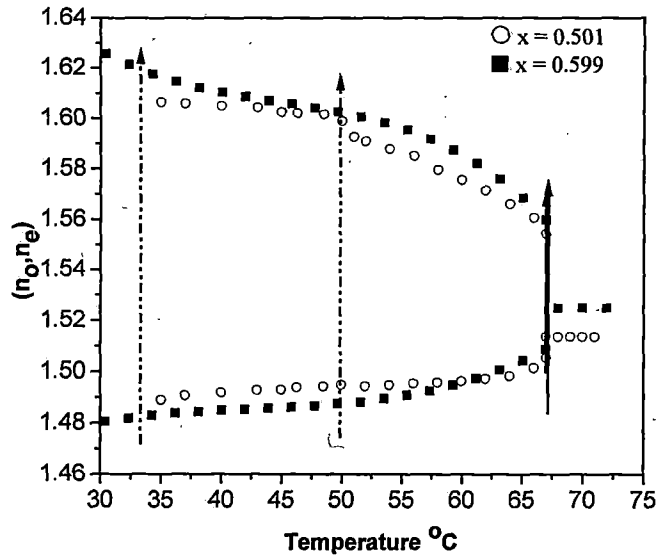


**FIGURE 5.5 (d).** Temperature variation of refractive indices ($n_o$, $n_e$) for ○ x = 0.501,■ x = 0.599. ↑ nematic – isotropic and ↑ smectic $A_d$ – nematic transition temperatures

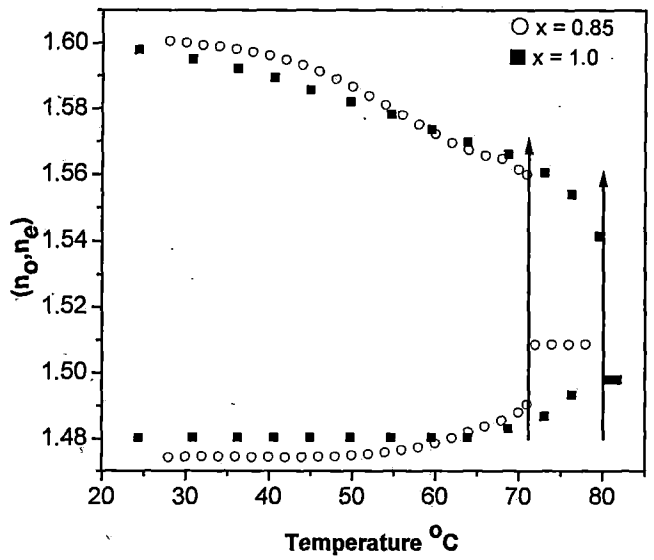


**FIGURE 5.5 (e).** Temperature variation of refractive indices ($n_o$, $n_e$) for ○ x = 0.85, ■ x = 1.0 (CPPCC). ↑ nematic – isotropic and ↑ smectic $A_d$ – nematic transition temperatures

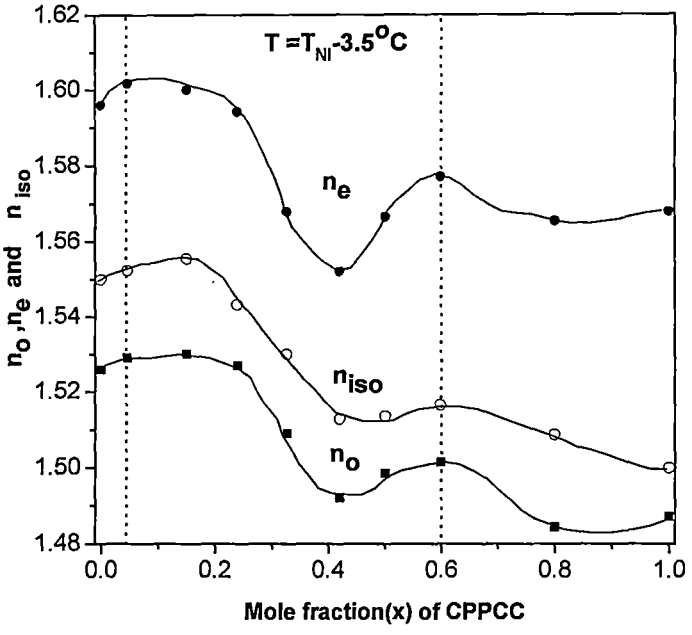


**FIGURE 5.6.** Variation of refractive indices ■ $n_o$, ● $n_e$, and ○ $n_{iso}$ with concentration; ↑ represents the induced smectic $A_d$ concentration range.

The variation of refractive indices $n_o$, $n_e$ at temperature $T=T_{NI}-3.5°C$ and $n_{iso}$ with mole fraction is shown in figure 5.6. For mixtures with $x < 0.24$ the $n_o$, $n_e$ and $n_{iso}$ values are more or less constant. However, these values decreases with increase in the molar concentration of $x > 0.24$ and shows a broad minimum near $x = 0.4$.

Principal molecular polarizability ($\alpha_o$, $\alpha_e$) is measured from refractive indices ($n_o$, $n_e$) by using Neugebauer's method [discussed in chapter 2]. The orientational order parameter $<P_2>$ is calculated using

$$< P_2 >= \frac{\alpha_e - \alpha_o}{\alpha_{\parallel} - \alpha_{\perp}} \qquad \textbf{5.1}$$

where $\alpha_o$ and $\alpha_e$ are respectively the effective polarizability for extraordinary and ordinary rays; and $\alpha_{||}$ and $\alpha_{\perp}$ are the polarizabilities

parallel and perpendicular to the long axis of the molecule. The polarizability anisotropies in the perfectly ordered state are determined by Haller's extrapolation method [as discussed in chapter 2] and the values for different concentrations (x) of this mixture are indicated in Table 5.1.

## 5.7 X-ray diffraction measurements:

X-ray diffraction patterns were recorded throughout the mesomorphic range. A magnetic field of 0.5T was applied to align the samples. The x-ray diffraction intensity data were analysed to evaluate order parameters using a procedure described in chapter 2. Layer thickness and the apparent molecular length in smectic and nematic phases were also determined from x-ray data. Plate 5.1 shows the x-ray diffraction photographs of the oriented sample of mixture x = 0.501 in the induced smectic (32°C) and nematic phases (44°C). The angular distributions of the x-ray intensity along the outer arc of the diffraction pattern, after necessary background correction, was used to determine orientational order parameter following equation 2.17, which has been described in chapter 2.

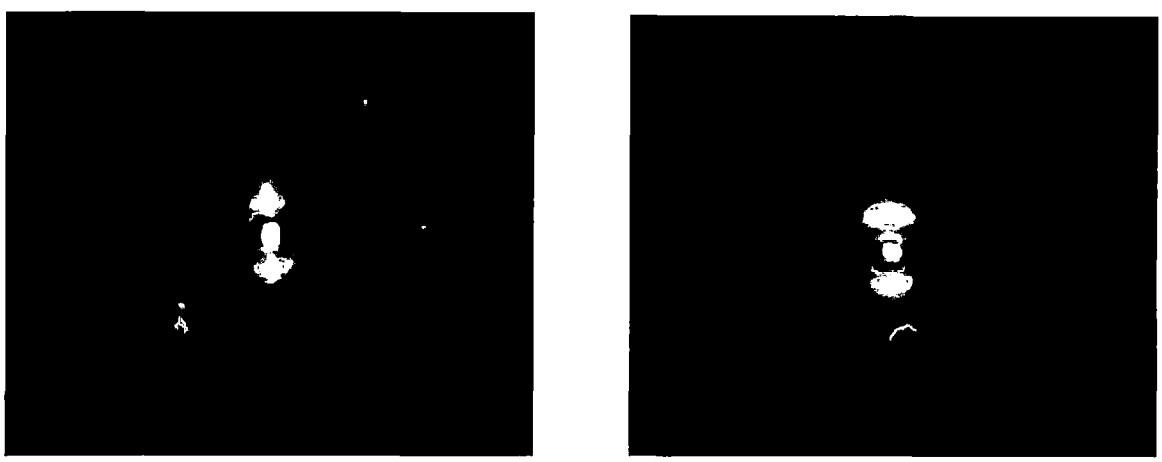

**(a)** **(b)**

**Plate 5.1:** X-ray diffraction photograph of the oriented sample **(a)** $SmA_d$ at T=32°C for x=0.501 **(b)** nematic phase at T=44°C for x=0.501.

Figure 5.13 – 5.22 show the variation of experimentally determined orientational order parameters (OOP) $\langle P_2 \rangle$ and $\langle P_4 \rangle$ with temperature for the system studied by x-ray diffraction measurement. In the same figures, I have plotted the $\langle P_2 \rangle$ values obtained from refractive index studies.

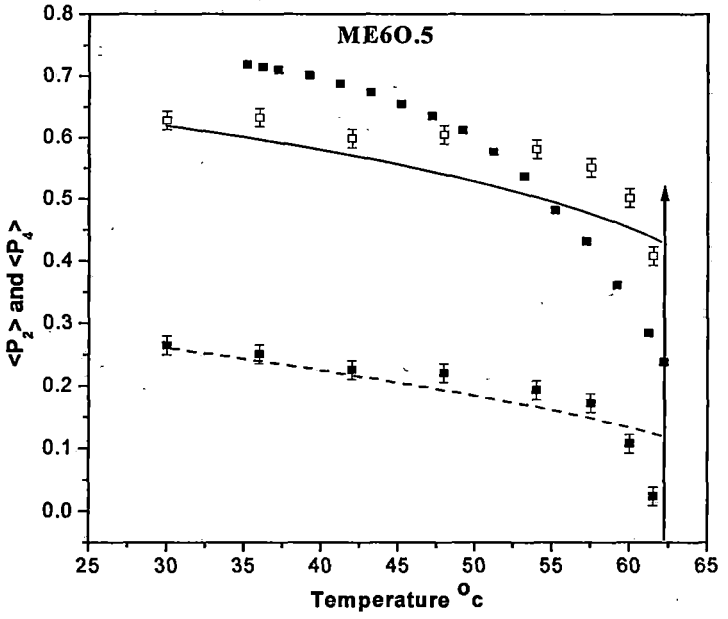


**FIGURE 5.13:** Temperature variation of $\langle P_2 \rangle$ for ME6O.5 determined from ■ refractive index, □ x-ray measurements; — $\langle P_2 \rangle$ and -- $\langle P_4 \rangle$ from Maier-Saupe theory. ↑ nematic – isotropic transition temperatures.

The $\langle P_2 \rangle$ values measured from x-ray diffraction studies are somewhat smaller than those obtain from refractive index measurements for all the mixtures except near the nematic isotropic phase transition.

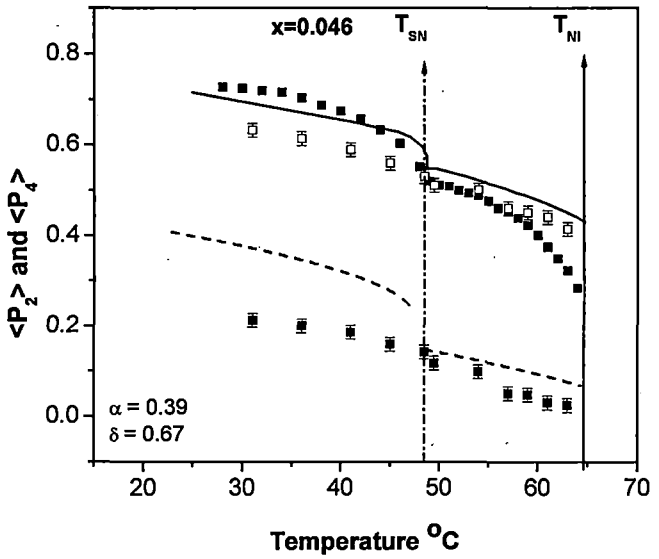


**FIGURE 5.14:** Temperature variation of $\langle P_2 \rangle$ for x=0.046 determined from ■ refractive index, □ x-ray measurements; — $\langle P_2 \rangle$ and -- $\langle P_4 \rangle$ from McMillan's theory. ↑ nematic – isotropic and ↑ smectic $A_d$ – nematic transition temperatures.

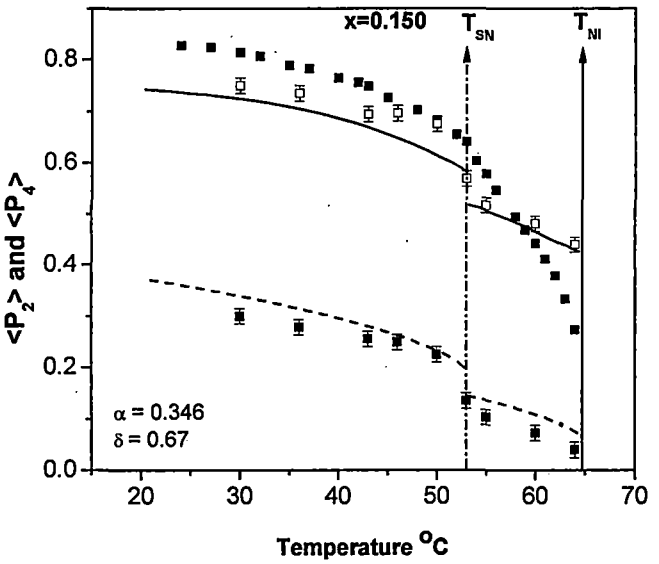


**FIGURE 5.15:** Temperature variation of $\langle P_2 \rangle$ for x=0.15 determined from ■ refractive index, □ x-ray measurements; — $\langle P_2 \rangle$ and -- $\langle P_4 \rangle$ from McMillan's theory. ↑ nematic – isotropic and ↑ smectic $A_d$ – nematic transition temperatures.

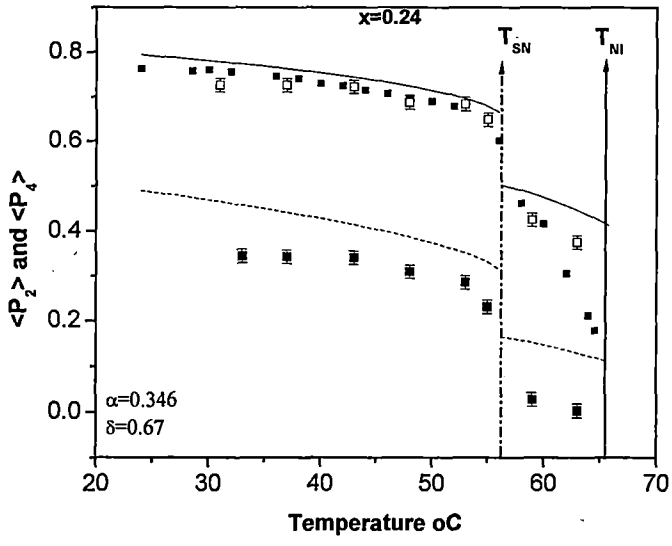


**FIGURE 5.16:** Temperature variation of $<P_2>$ for x=0.24 determined from ■ refractive index, □ x-ray measurements; — $<P_2>$ and -- $<P_4>$ from McMillan's theory. ↑ nematic – isotropic and ↑ smectic $A_d$ – nematic transition temperatures.

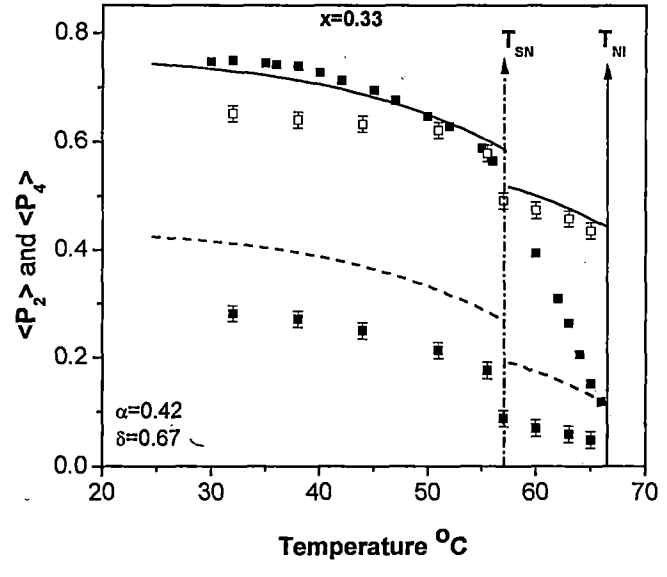


**FIGURE 5.17:** Temperature variation of $<P_2>$ for x=0.33 determined from ■ refractive index, □ x-ray measurements; — $<P_2>$ and -- $<P_4>$ from McMillan's theory. ↑ nematic – isotropic and ↑ smectic $A_d$ – nematic transition temperatures.

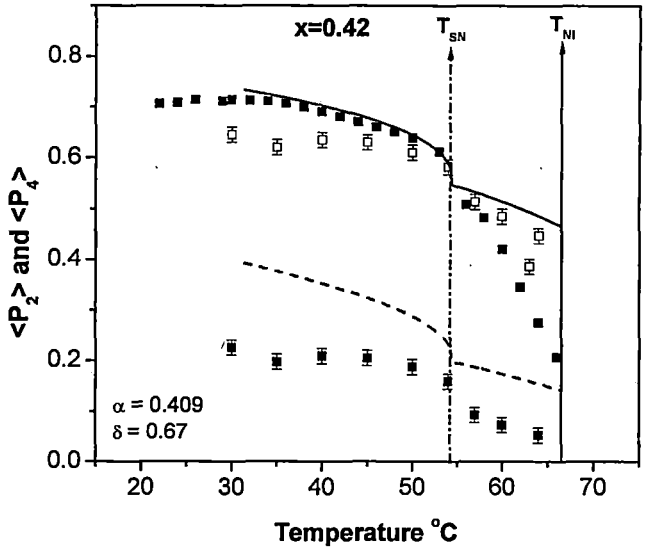


**FIGURE 5.18:** Temperature variation of <$P_2$> for x=0.42 determined from ■ refractive index, □ x-ray measurements; — <$P_2$> and -- <$P_4$> from McMillan's theory. ↑ nematic – isotropic and ↑ smectic $A_d$ – nematic transition temperatures

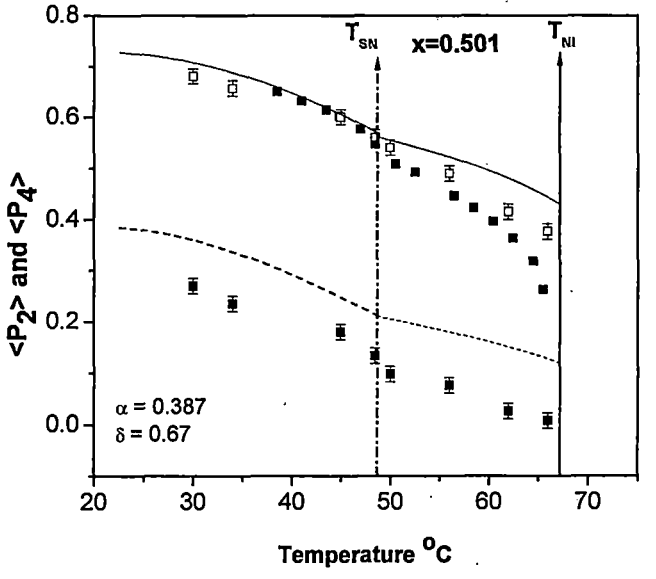


**FIGURE 5.19:** Temperature variation of <$P_2$> for x=0.501 determined from ■ refractive index, □ x-ray measurements; — <$P_2$> and -- <$P_4$> from McMillan's theory. ↑ nematic – isotropic and ↑ smectic $A_d$ – nematic transition temperatures.

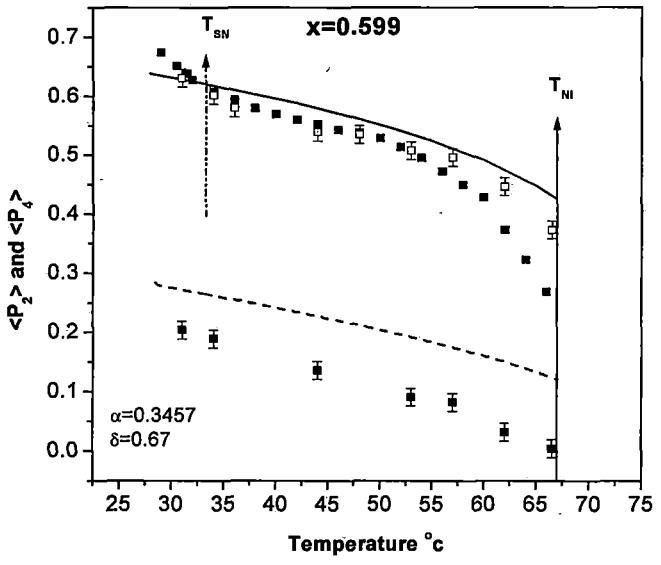


**FIGURE 5.20:** Temperature variation of $\langle P_2 \rangle$ for x=0.599 determined from ■ refractive index, □ x-ray measurements; — $\langle P_2 \rangle$ and -- $\langle P_4 \rangle$ from McMillan's theory. ↑ nematic – isotropic and ↑ smectic $A_d$ – nematic transition temperatures.

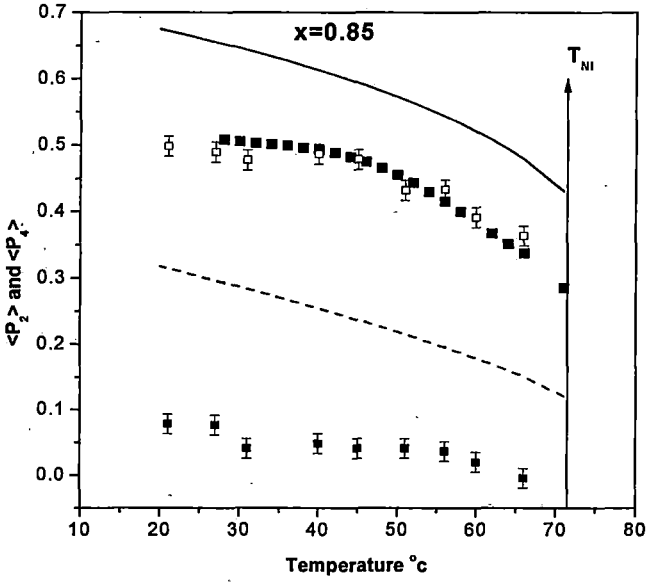


**FIGURE 5.21:** Temperature variation of $\langle P_2 \rangle$ for x=0.85 determined from ■ refractive index, □ x-ray measurements; — $\langle P_2 \rangle$ and -- $\langle P_4 \rangle$ from Maier-Saupe theory. ↑ nematic – isotropic and ↑ smectic $A_d$ – nematic transition temperatures.

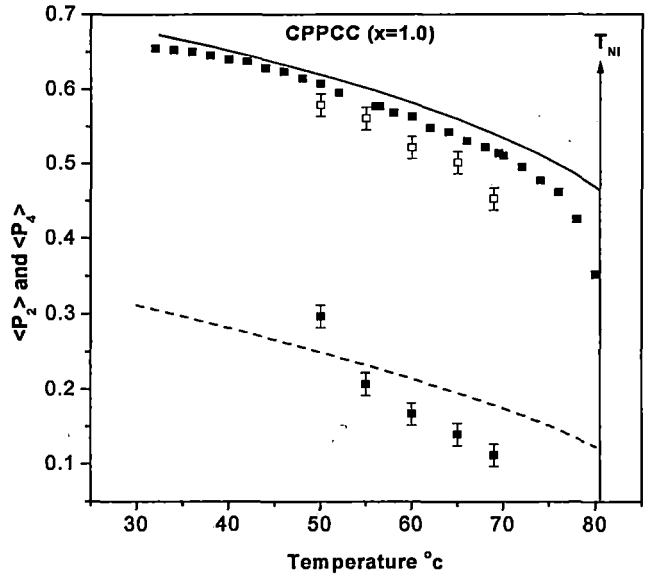


**FIGURE 5.22:** Temperature variation of $\langle P_2 \rangle$ for CPPCC determined from ■ refractive index, □ x-ray measurements; — $\langle P_2 \rangle$ and -- $\langle P_4 \rangle$ from Maier-Saupe theory. ↑ nematic – isotropic transition temperatures.

From the temperature dependences of the orientational order parameters for mixtures at different concentration it is again observed that there is an appreciable change in the order parameter value at the smectic $A_d$ to nematic phase transition temperature for mixtures around $x \approx 0.33$.

I have also fitted the experimental order parameter values with McMillan's theory [12] for mixtures having smectic $A_d$ phase using $\alpha$ and $\delta$ as adjustable parameters in the McMillan potential. It may be mentioned that the order parameter values has been calculated keeping constant $\delta$ values over the entire composition range. The best fitted theoretical curve and the values of $\alpha$ and $\delta$ used for this calculations are shown in the respective figures. It is to be noted here that, x-ray diffraction photographs of mixtures having 0.15, 0.24 mole fractions of CPPCC were found to exhibit second order

meridional reflections from the smectic layers implying rather high translational order. Orientational order parameter values from x-ray diffraction measurement are also found to be relatively high for these mixtures. The agreement between the experimental $\langle P_2 \rangle$ values from x-ray diffraction measurements with those calculated from McMillan's theory is fair for x = 0.15 and excellent for x = 0.24 (figure 5.15 – 5.16). Also, there is a discrete change in the values of $\langle P_2 \rangle$ and $\langle P_4 \rangle$ at the smectic-nematic phase transition, indicating a first order phase transition for these mixtures.

The mixtures having x = 0.33 and 0.42 do not show second order meridional reflection (as observed from x-ray diffraction photographs) but these mixtures exhibit first order smectic-nematic phase transition as seen from the discontinuity in OOP values at the transition (figure 5.17 – 5.18). The best fitted theoretical curve for the McMillan's theory is also indicated in these figures. For mixtures having mole fraction x = 0.046, 0.501 and 0.599, the experimental order parameter values seem to change continuously at the S/N transition and their agreement with McMillan's theory is fair for x = 0.5 and 0.599; and poor for x = 0.046. Mixture with mole fraction 0.85 has only nematic phase; hence the experimental $\langle P_2 \rangle$ and $\langle P_4 \rangle$ values have been compared with the theoretical Maier-Saupe values.

In the nematic phase of the mixtures which exhibit induced Smectic $A_d$ phase, the experimental OOP values determined from x-ray diffraction study are in closer agreement with the theoretical curve compared to that obtained from refractive index measurement. But there is disagreement near the nematic-isotropic transition temperature. This discrepancy may be due to the fact that different approximations and averaging are involved in calculating

orientational order parameter from experimental data obtained from x-ray studies in one hand and birefringence measurements on the other hand [13]. The $\langle P_4 \rangle$ values obtained from x-ray diffraction measurement however, is always significantly less than the theoretically calculated values in both smectic and nematic phases. Such behaviour of $\langle P_4 \rangle$ has been observed by others [14-16].

Figure 5.23 shows the variation of OOP values at T=35°C against mole fraction from x-ray diffraction measurements. The Δn values at the same temperature are also plotted in this figure. From this figure it is clear that in the smectic phase the OOP values initially increases with molar concentration upto x = 0.24 and then decreases and showing a broad minima around x = 0.4. The Δn values also show similar behaviour. Previous workers have also observed similar trend in the variation of $\langle P_2 \rangle$ and birefringence with mole fraction for a binary mixture ME6O.5 and a

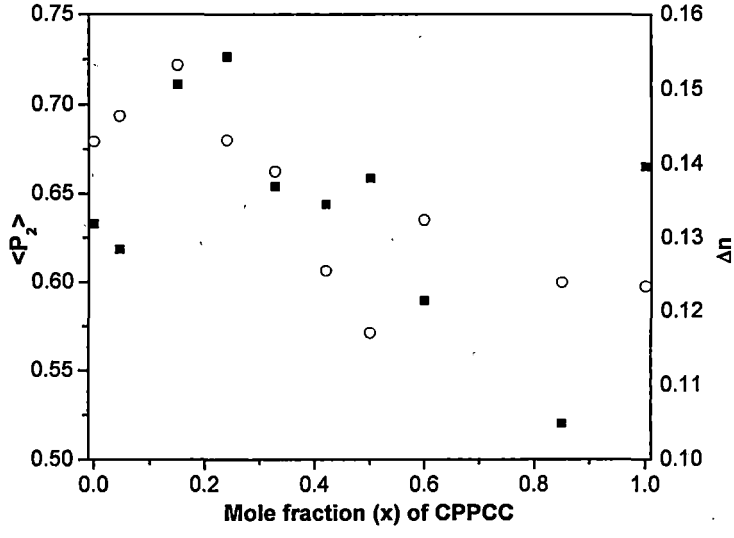


**FIGURE 5.23:** Concentration variation of $\langle P_2 \rangle$ values obtained form x-ray diffraction measurement and Δn values at T=35°C.

a cyanobiphenyl (5CB) as the individual components. However, for such system this minimum has been observed for nearly equimolar concentration [4].

Regarding the behaviour of entropy change associated with the smectic – nematic phase transition, $\Delta S_{SN}$ in this system, I have calculated $\Delta S_{SN}$ from McMillan's theory, taking the values of $\alpha,\delta,\eta,\tau$ and $\sigma$ , at either side of the smectic nematic transition temperature obtained from the best fit theoretical curve to the experimental x-ray $\langle P_2 \rangle$ data. The $\Delta S_{SN}=(S_N-S_S)$ is calculated from the following well-known expressions [17].

$$S_S = -\frac{Nk}{T^*}(\eta_S^2 + \alpha\delta\tau_S^2 + \alpha\sigma_S^2) + Nk \ln Z_S \qquad \textbf{5.1}$$

$$S_N = -\frac{Nk}{T^*}\eta_N^2 + Nk \ln Z_N \qquad \textbf{5.2}$$

where $T^* = \frac{kT}{\nu}$

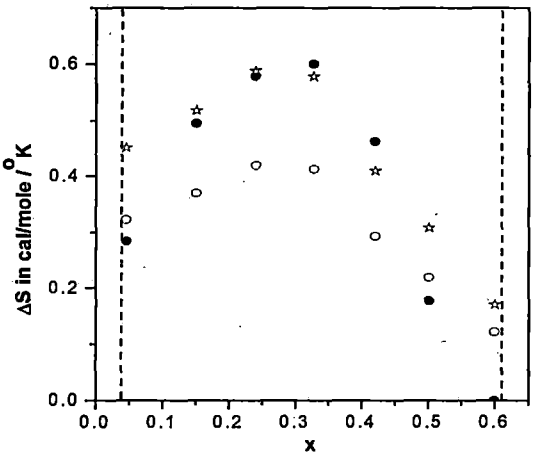


**FIGURE 5.24:** Entropy change associated with smectic to nematic phase transition of mixture ME6O.5/CPPCC with mole fraction. ○ calculated values of $\Delta S_{SN}$ from McMillan's theory. ☆ calculated values multiplied by a factor 1.4; ● experimental values.

Figure 5.24 shows the theoretically estimated and experimentally determined entropy values. It is observed that, although the general trend of the behaviour of entropy change at the smectic $A_d$ – N phase transition, $\Delta S_{SN}$, in the region of the induced smectic phase is reproduced by the theory, the calculated values of the entropy change at the smectic to nematic transition are somewhat 1.4 times larger. The agreement could have been better by changing the values of $\alpha$ and $\delta$, but I have used only those values which give best fit to our experimental order parameter values.

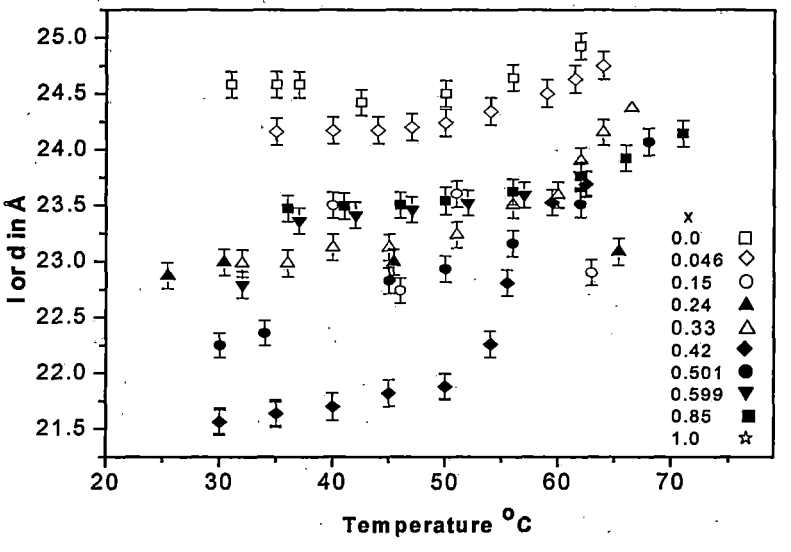


**FIGURE 5.23:** Temperature variation of apparent molecular length in the nematic phase and the layer thickness in the smectic phase.

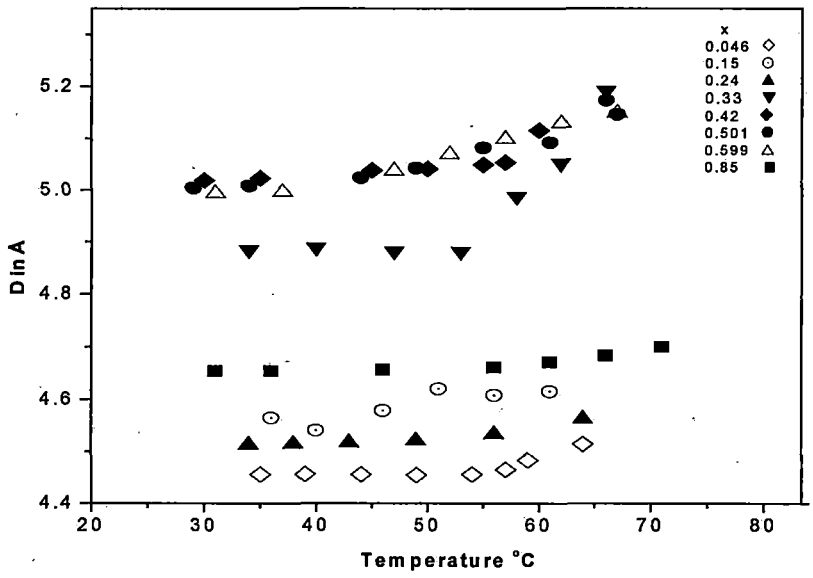


**FIGURE 5.24:** Lateral intermolecular distance (D) at different temperatures for mixtures of ME6O.5 + CPPCC.

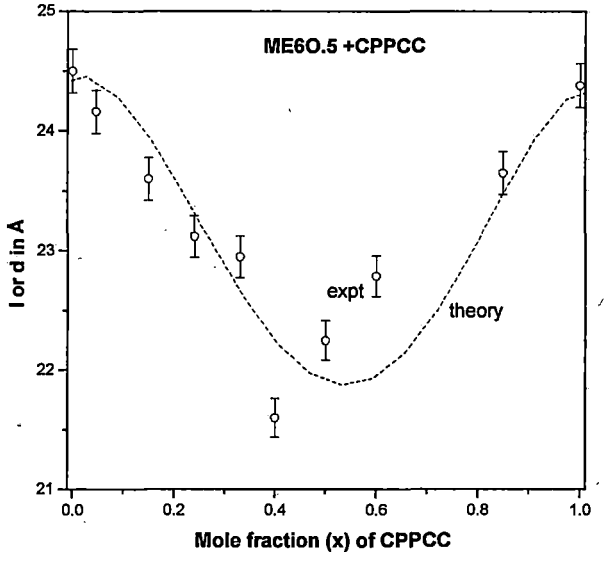


**FIGURE 5.25:** Variation of layer thickness (d) with molar concentration. Vertical bar represent the estimated error.

The temperature variation of the layer thickness for the mixtures is shown in figure 5.23. It can be seen that the layer thickness (d) values are almost independent of temperature. This is quite common in smectic A phases.

However, the apparent molecular lengths (l) in the nematic phase increases with increasing temperature.

The temperature variation of lateral intermolecular distance (D) for all the mixtures is shown in figure 5.24. It is seen that D values are almost constant throughout the mesophase except near the clearing temperature.

The composition variation of layer thickness at 35°C is shown in figure 5.25. The variation shows a broad minimum of ~21.6Å at about x=0.42 concentration. This behaviour is also observed by Das et al [4-6], where the layer thickness shows a minimum at about equimolar concentration. In order to calculate the variation of layer thickness with molar concentration we assume that the pure CPPCC molecules (molecule A) form association in the nematic phase. The apparent molecular length of CPPCC as determined from x-ray diffraction studies is 24Å, which is much larger than its model molecular length of 17Å. It is considered that the molecules form association and the pure state is a mixture of predominantly associated dimers and monomers, which are in dynamic equilibrium. On the other hand, since the apparent molecular length of ME6O.5 molecule (molecule B), as determined from x-ray studies [4], is almost equal to the model molecular length, so the molecule B exists as a monomer in its pure state. In mixtures we can assume that the terminal polar molecules form homo dimers (AA) as well as hetero dimmers (AB). The possibility of formation of such homo and hetero complexes was proposed earlier by Dabrowski et al. [18]. Garg and Spears from their molecular modeling on a related system showed a strong interaction between two species forming hybrid molecule [19]. Such cross

interaction is also proposed by Kyu et al [20-21] from their theoretical work on induced smectic A phase.

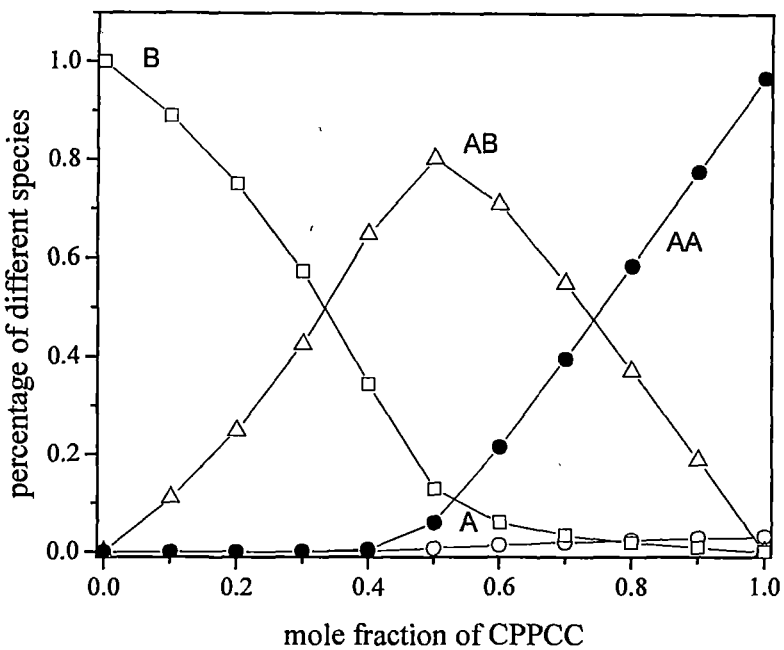


**FIGURE 5.26:** Percentage of different species A, B, AB and AA as a function of mole fraction of CPPCC.

Hence in the mixtures we can assume that there exist A, B, AA and AB types of molecules in equilibrium. The mole fractions of different species $x_A$, $x_B$, $x_{AA}$ and $x_{AB}$ can be determined from the equilibrium constants $K_A$ and $K_{AB}$ for the associations, $A + A \leftrightarrow AA$, $A + B \leftrightarrow AB$, respectively. Using equilibrium constants $K_A = 1000$ and $K_{AB} = 800$, the percentage of different species, A, B, AA and AB as function of mole fraction of CPPCC, have been calculated, which is shown in Figure 5.26. These values of $K_A$ and $K_{AB}$ are typical of similar systems we have studied previously [22].

The average d value may then be written as

$$d = x_A d_A + x_{AA} d_{AA} + x_{AB} d_{AB} + x_B d_B \qquad \textbf{5.3}$$

where $x_A$, $x_B$, $x_{AA}$, $x_{AB}$ are mole fractions of respective components in chemical equilibrium, $d_A$ and $d_B$ are taken to be equal to the lengths of the molecules A and B as obtained from molecular model kit. $d_{AB}$ is taken as the arithmetic mean $d_A$ and $d_B$, while $d_{AA}$ has been adjusted so that in pure terminal polar compound, which has both A and AA molecules, the apparent molecular length equals ($= x_A d_A + x_{AA} d_{AA}$) the experimentally observed d value. The values of d at T = 35° C, calculated from equation (5.3) is shown in Figure 5.25. It is to be noted that the values of $K_A$ and $K_{AB}$ can be varied by about 15% without much change in the calculated values of d. From figure 5.25 it is seen that the calculated result for the layer thickness is in excellent agreement with the experimental values.

In figure 5.27 I have also plotted the average lateral distance between the molecules at T=35°C with molar concentration. Interestingly, it is seen that D values are more or less constant for $x<0.24$ and then increases showing a maximum near equimolar concentration.

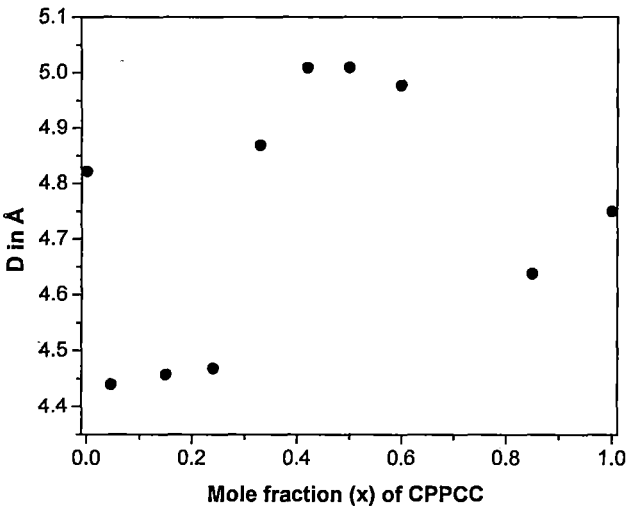


**FIGURE 5.27:** Variation of lateral intermolecular distance (D) with molar concentration.

## 5.8 Permittivity measurements:

The temperature variations of the dielectric permittivities ($\varepsilon_{\parallel}$ and $\varepsilon_{\perp}$) are shown in figures 5.28(a)-5.28(c). There is no sharp discontinuity in the measured permittivity components for the mixtures as well as pure compounds at the nematic to isotropic transition. The mixtures and the pure compounds exhibit positive dielectric anisotropy. Dielectric anisotropy ($\Delta\varepsilon$) is large for pure CPPCC and this is due to the terminal polar CN group. On the other hand $\Delta\varepsilon$ for non-polar ME6O.5 is very small. The isotropic dielectric permittivity ($\varepsilon_{iso}$) and the average dielectric permittivity $\bar{\varepsilon} = \{1/3(\varepsilon_{\parallel} + 2\varepsilon_{\perp})\}$ of this mesogen almost coincide at the nematic-isotropic phase transition temperature, as predicted by Madhusudana and Chandrasekhar [23].

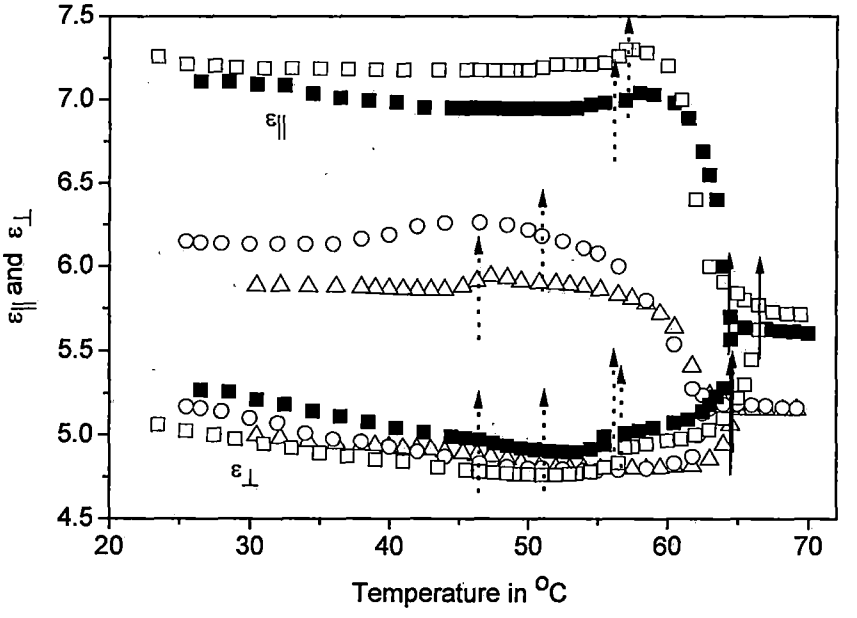


**FIGURE 5.28 (a):** Variation of electric permittivity as a function of temperature: Δ (x= 0.046); o (x= 0.15); ■ (x= 0.24); □ (x=0.33). ↑ for nematic to isotropic transition; ↑ for smectic $A_d$ to nematic transition.

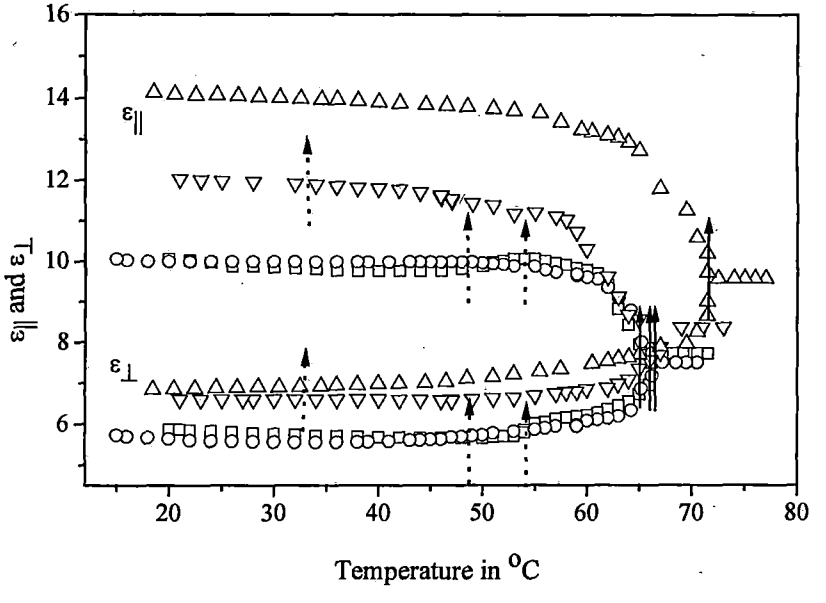


**FIGURE 5.28 (b):** Variation of electric permittivity as a function of temperature: □ (x= 0.42);o (x= 0.5); ▽ (x= 0.6); Δ (x=0.85). ↑ for nematic to isotropic transition; ↑ for smectic $A_d$ to nematic transition.

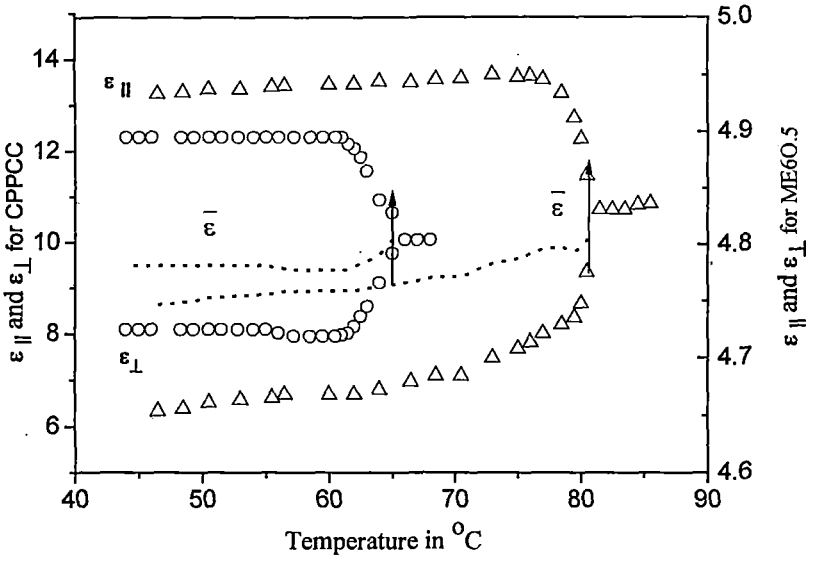


**FIGURE 5.28 (c):** Variation of electric permittivity as a function of temperature for the pure compounds: o ME 6O.5; Δ CPPCC. ↑ for nematic to isotropic transition.

The value of the isotropic dielectric permittivity ($\varepsilon_{iso}$) of the mixtures extrapolated to the nematic phase is greater than the average dielectric permittivity. Mixtures with mole fraction x in the vicinity of 0.3, show a discontinuity in the permittivity components at the smectic-nematic transitions. The value of both the dielectric permittivity components reduces in the smectic phase. This reduction is maximum when x is near about 0.3. Incidentally, these mixtures correspond to that region of the phase diagram where the induced smectic $A_d$ phase is most stable. Similar effects have been observed in mixtures of 5CB and ME5O.5 [6]. For other mixtures there is no longer such a discontinuity in the permittivity components at the smectic-nematic transitions.

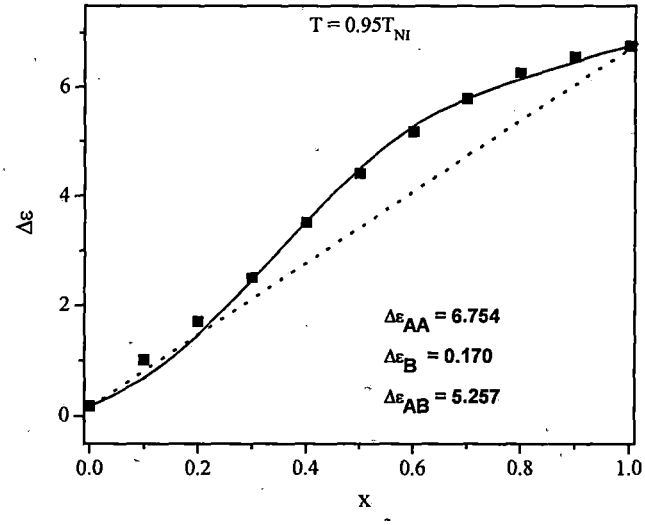


**FIGURE 5.29:** The permittivity anisotropy Δε plotted against mole fraction (x) at a reduced temperature, $T_R = 0.95$. ■ experimental values, Solid line represents the calculated values. Dotted line represents the average values.

In Figure 5.29 I have plotted Δε as a function of mole fraction of CPPCC corresponding to a reduced temperature $T_R = (T/T_{NI}) = 0.95$. At this reduced temperature all the mixtures with mole fractions $0.03<x<0.6$ show $SmA_d$ phase. The Δε values having mole fractions $x > 0.2$ lie significantly above the average values, shown by a straight line connecting those of the pure compounds.

Similar to the assumptions made in the calculation of the smectic layer spacings (d) as discussed previously in this chapter, in order to calculate the variation of Δε with molar concentration, it is again assumed that the molecules form association and the pure state is a mixture of predominantly associated dimers and monomers, which are in dynamic equilibrium. The percentage of different species has already been shown in figure 5.26.

The average values of $\Delta\varepsilon$ may then be written as

$$\Delta\varepsilon = x_A\Delta\varepsilon_A + x_{AA}\Delta\varepsilon_{AA} + x_{AB}\,\Delta\varepsilon_{AB} + x_B\Delta\varepsilon_B \qquad \textbf{5.4}$$

From 5.26 it is apparent that in pure CPPCC only 3% of A monomers are present. In mixtures this value gradually decreases with decrease in the mole fraction of CPPCC and is nearly absent around $x \approx 0.5$. Since I am not in a position to calculate $\Delta\varepsilon_A$, in this calculation I assumed $\Delta\varepsilon_A \approx \Delta\varepsilon_{AA}=5.57$ (i.e. the experimentally determined $\Delta\varepsilon$ value of pure CPPCC at $T_R = 0.95$). I have assumed $\Delta\varepsilon_B$ is the dielectric anisotropy for ME6O.5 at $T_R = 0.95$. However, I still do not know the value of $\Delta\varepsilon_{AB}$, which may be estimated as follows:- From figure 5.26 it is evident that for mixture with $x \approx 0.4$ there is no A monomer and about 70% of the molecules are forming AB dimer. Knowing the experimental value of $\Delta\varepsilon$ at $T_R = 0.95$, I have estimated $\Delta\varepsilon_{AB}$ for AB dimer from equation 5.4.

$$\Delta\varepsilon = \Delta\varepsilon_{AA}\,x_{AA} + \Delta\varepsilon_{AB}\,x_{AB} + \Delta\varepsilon_B\,x_B \qquad \textbf{5.5}$$

From this calculation, $\Delta\varepsilon_{AB}$ is estimated to be 5.258 at the reduced temperature, $T_R = 0.95$.

The values of $\Delta\varepsilon$ at $T_R = 0.95$, calculated from equation 5.5 is shown in figure 5.29. It is to be noted that the values of $K_A$ and $K_{AB}$ can be varied by about 15% without any appreciable change in the calculated values of $\Delta\varepsilon$. From Figure 5.29 it is seen that the calculated result for the dielectric anisotropy is in excellent agreement with the experimental values.

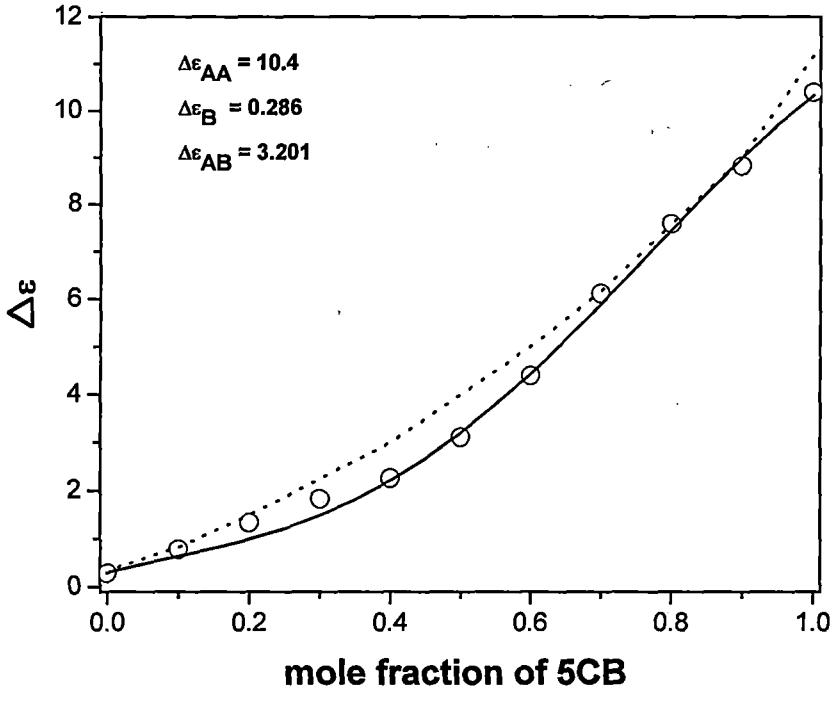


**FIGURE 5.30:** The dielectric anisotropy Δε in the nematic phase plotted against mole fraction of 5CB (x) at a reduced temperature, $T_R$ = 0.99 for binary mixture ME5O.5 + 5CB. The open circles are experimental points and the solid line represents the calculated values. Dotted line represents the calculated values using additive rule by Dunmur *et al.* [2].

Previously, Das et al have successfully explained the variation of layer thickness with molar concentration by assuming the formation of two types of dimers in a related mixture of 5CB and ME50.5 showing induced smectic $A_d$ phase [6]. Extending this work to explain the molar concentration dependence of the dielectric anisotropy of the same mixture (5CB + ME5O.5) as reported by Dunmur et al [7], it is observed that the results of this calculations using equation 5.5 are also in good agreement with the experimentally determined values as shown in figure 5.30.

These results once again prove the validity of the model of formation of molecular associations in the form of homo and hetero dimers in polar – non polar mixtures exhibiting induced smectic $A_d$ phases [22].

Table 5.1: Polarizability anisotropy calculated from Haller's extrapolation procedure for different mixtures

| x | $(\alpha_{\|\|} - \alpha_{\perp}) \times 10^{-24}$ |
|---|---|
| 0.046 | 16.75 |
| 0.24 | 14.26 |
| 0.33 | 14.845 |
| 0.42 | 14.99 |
| 0.15 | 15.50 |
| 0.501 | 15.265 |
| 0.599 | 15.40 |
| 0.85 | 17.508 |

**References:**


1. C. S. Oh, *Mol. Cryst. Liq. Cryst.*, **42**, 1(1977).
2. B. Engelen and F. Schneider, *Z. Naturforsch*, **33a**, 1077 (1978).
3. M. Domon and J. Billard, *J. Phys, (Paris)*, **40**, C3-413 (1979).
4. M.K. Das and R. Paul, *Phase Transitions*, **46**, 185(1994), **48**, 255(1994).
5. M.K. Das, R. Paul , *Mol. Cryst. Liq. Cryst.*, **260**, 477(1995).
6. M.K. Das, R. Paul and D.A. Dunmur, *Mol. Cryst. Liq. Cryst.*, **285**, 239 (1995).
7. D.A. Dunmur, R.G. Walker and P. Palffy-Muhoray, *Mol. Cryst. Liq. Cryst.*, **122,** 321(1985).
8. M. Domon and J. Billard, *J. Phys, (Paris)*, **40**, C3-413 (1979).
9. F. Schneider and N.K. Sharma, *Z. Naturforsch.*, **36a**, 62, (1981).
10. K. Araya and Y. Matsunaga, Bull. *Chem. Soc. Jap.*, **53**, 3079 (1980).
11. M. Brodzik and R. Dabrowski, *Mol. Cryst. Liq. Cryst.*, **260**, 361(1995).
12. W. L. McMillan, *Phys. Rev.*, **A4**, 1236 (1971), **A6**, 936 (1972).
13. M.K. Das and R. Paul, *Mol. Cryst. Liq. Cryst.*, 239 107(1994).
14. M. Mitra and R. Paul, *Mol. Cryst. Liq. Cryst.*, 177, 71 (1989).
15. M. Mitra, S. Paul and R. Paul, *Liq. Cryst.*, **3**, 123 (1988).
16. P. Mandal, M. Mitra, S. Paul and R. Paul, *Liq. Cryst.*, **2**, 183 (1987).
17. P. J. Wojtowicz, "*Introduction to Liquid Crystals*", (Eds.) E. B. Priestely, P. J. Wojtwicz and P. Sheng, Plenum Press, New York, p. 95 (1947).

18. R. Dabrowski, K. Czuprynski, "*Modern topics in Liquid Crystals - from Neutron Scattering to Ferroelectricity*", (Ed.) Agnes Buka, World Scientific, 1993 (London).
19. Shila Garg and Tom Spears, *Mol. Cryst. Liq. Cryst.*, 409, 335 (2004).
20. Thein Kyu, Hao-Wen Chiu and Tisato Kajiyama, *Phy. Rev.* **E55**, 7105 (1997).
21. Hao-Wen Chiu and Thein Kyu, *J. Chem. Phys*, **103**, 7471 (1995).
22. M. K. Das, R. Paul , *Mol. Cryst. Liq. Cryst.*, **260**, 477 (1997).
23. N. V. Madhusudana, K.L. Savithramina and S. Chandrasekhar, *Pramana*, **8**, 22 (1977).